International Journal of Fracture (2006) 139:537–544
DOI 10.1007/s10704-006-0101-8

THREE_DIMENSIONAL SIMULATION OF FRACTURE BEHAVIOR OF ELASTIC-BRITTLE MATERIAL WITH INITIAL CRACK PATTERN

V.A. Romanova[*], *R.R. Balokhonov, P.V. Makarov*
Institute of Strength Physics and Materials Science, SB RAS, pr. Academicheskii 2/1, 634021, Tomsk, Russia
[*]*E-mail varvara@ispms.tsc.ru*

Abstract. Numerical simulation of mechanical behavior of heterogeneous materials under loading with an explicit consideration for their 3D mesoscale structure is given. A 3-D problem in the dynamic formulation is solved using the finite-difference method. As an example, a coal specimen under tension and compression is examined, with an initial crack pattern taken into account. It is been shown that the fracture criterion we used in the calculations provides adequate description of fracture behavior under tension and compression on both macro and mesoscale level.

Keywords: Computational mechanics, cracks, 3D-structure, coal

1. Introduction. Earlier (Romanova et al. 2003, 2004, 2005), we simulated the elasto-plastic behavior of materials with explicit consideration for their 3-D structure and utilized a special procedure of introducing 3-D heterogeneities. Stress and strain evolution in polycrystalline materials and composites under tension, compression and shock wave loading has been numerically studied.

Here, we apply this approach to simulation of fracture of a coal specimen. A classical fracture criterion based on the maximum equivalent stress (Kachanov, 1974, Cherepanov, 1979) was modified to describe crack evolution on the mesoscale level. Kachanov (1974) noted that, for homogeneous materials, this criterion may not be adequate for brittle fracture. Balokhonov (2005) showed, however, that an explicit introduction of a material structure makes this criterion adequate. It has been demonstrated (Balokhonov (2005)) for a metal-matrix composite structure subjected to tension and compression that due to its heterogeneity the material on the mesoscale level exhibits complex stress-strain behavior so that at any method of external load application in the vicinity of interfaces there can be found areas undergoing tension, compression, shear, rotation and their combination. Taking into account that the tensile strength of brittle materials is, as a rule, lower then the compressive one, most cracks on the mesoscale level originate in the areas of tensile or shear deformation even if the applied loads are compressive.

We simulate fracture process on the mesoscale level, with the initial crack pattern generated by a step-by-step packing (SSP), see Romanova et al (2003, 2004, 2005). The main goal is to study numerically crack evolution in the coal specimen under tension and compression and to examine the applicability of the maximum equivalent stress theory in the 3D-simulation of brittle fracture.

2. Mathematical formulation

System of equations: Assuming that a medium under deformation remains continuous at the meso- and macro-scale levels, with the damaged areas characterized by a reduced strength, we use methods of continuum mechanics. Since individual cracks can propagate at speeds comparable to the speed of sound, the problem is solved in the dynamic formulation. Differential equations include the equation of continuity

$$\frac{\dot{V}}{V} - U_{i,i} = 0 \tag{1}$$

the equation of motion

$$\rho \dot{U}_i = \sigma_{ij,j}, \tag{2}$$

and the expression for stress tensor components

$$\sigma_{ij} = -P\delta_{ij} + S_{ij}, \tag{3}$$

where $i = 1,2,3$, $j = 1,2,3$; $U_i = \dot{x}_i$, U_i and x_i are the velocity vector components and Cartesian coordinates, respectively; $V = \rho_0/\rho$ is the relative volume; ρ_0 and ρ are the reference and current densities; δ_{ij} is the Kronecker delta. The upper dot denotes a time derivative.

The pressure is defined from the linear barotropic equation

$$\mathrm{P} = -\mathrm{K}\varepsilon_{\mathrm{kk}}, \tag{4}$$

and the deviatoric stresses are written in the form of the Hook's law

$$\dot{S}_{ij}^{*} = 2\mu\left(\dot{\varepsilon}_{ij} - \frac{1}{3}\dot{\varepsilon}_{kk}\delta_{ij}\right), \tag{5}$$

where K and μ are the bulk and shear modules. The strain rate tensor is

$$\dot{\varepsilon}_{ij} = (1/2)\left(U_{i,j} + U_{j,i}\right). \tag{6}$$

Due to its efficiency, in comparison to other numerical techniques (variational-difference, Cherepanov, 2003, finite-elements, Astley, 1992), the finite-difference method developed by Wilkins et al (1975) has been chosen to solve the system (1)-(6)

Fracture model: Fracture criterion based on a maximum equivalent stress theory (Cherepanov, 1979, Kachanov, 1974) is applied to coal: fracture occurs when the equivalent stress σ_{eq} reaches its critical value:

$$\sigma_{eq} = \frac{1}{\sqrt{2}}\sqrt{S_{ij}S_{ij}} = \sigma^{*}, \tag{7}$$

where σ^{*} is the material tensile strength.

In order to take into account a difference in tensile and compressive strength magnitudes, specific for brittle materials (Cherepanov, 1979, Kachanov, 1974, Trubitsyn et al., 2002, criterion (7) was modified as follows. If $\varepsilon_{kk} > 0$, material fails locally if the local equivalent stress σ_{eq} reaches tensile strength, whereas if $\varepsilon_{kk} < 0$,

fracture surface in the stress space is limited by the compressive strength value. Trubitsyn et al (2002) pointed out that the coal compressive strength is, as a rule, several times higher than the tensile one. Under further loading, if $\varepsilon_{kk} > 0$, failed regions are assumed to lose strength so that both deviatoric stress (5) and pressure (4) become zero. If local ε_{kk} is negative, the damaged material can resist only compressive loads, i.e. pressure is calculated by (4), while stress deviator (5) is zero.

Cherepanov (1979) and Kachanov (1974) noted that criterion (7) formulated in classical fracture mechanics for a homogeneous elasto-plastic material subjected to tension may not be adequate for brittle fracture. For heterogeneous media with explicitly introduced mesoscale structure, Balokhonov (2005) showed that the theory provides adequate results both for tension and compression. Due to the structural heterogeneity, there can be found local mesoscale areas undergoing compression, tension, shear, rotation and their combination, regardless of the method of external loading,. Thus, in any loading conditions there are mesoscale tensile areas in which fracture occurs in accordance with the maximum equivalent stress criterion (7).

Structure model, mechanical properties and loading conditions: Material meso-structure is introduced in the calculations via a spatial-dependent distribution of appropriate material properties, i.e. density, elastic modules, strength properties and etc., which is a non-trivial task in the case of three dimensions. In contrast to the 2D-problem, when 2D-structures can be derived from experimental metallographic images, there is no simple way to introduce a real 3D-structure since it requires to define structural patterns not only on the surface but also in the bulk of the specimen. The scanning techniques (e.g. Jensen (2002)) which allow one to obtain a series of layer-by-layer structural images are, as a rule, laborious and very expensive. It is a challenge, therefore, to design artificial 3D-structures similar to real those in shape, size and volume content of their components.

In the general case, the design of a 3D-structure is reduced to the problem of packing a finite volume with structure elements without gaps and overlapping. In the last few decades, several methods of computer-aided simulation of microscopic heterogeneities have been developed (see the review edited by Raabe et al. (2004)), including Potts Monte Carlo Method, Voronoi tessellation, cellular automata, pseudo-front tracking method, the phase-field approach etc.. Some of them use a geometrical procedure to generate regular or irregular structures and others are based on certain physical principles and thermodynamic formulations. All of these were originally applied in 2D-simulations and their main goal was to obtain reasonable conclusions regarding the kinetic and statistical aspects of a 2D grain growth. Although in recent works (Raabe et al. (2004)) some of these methods were successfully applied in a 3D case, realization of these techniques in three dimensions is for the most part a complicated task calling for optimization of computational algorithms since the memory and processing time requirements needed to make calculations increase dramatically with the increase of spatial dimensions.

In this paper, in order to design the coal structure whose mechanical behaviour will be further numerically investigated, use was made of a step-by-step packing (SSP) algorithm proposed by Romanova et al. (2003). In contrast to the methods listed in Raabe et al. (2004), this technique disregards physical and thermodynamical aspects of the microstructure evolution such as grain growth, phase coalescence, recrystallization and so on. The main idea is to pack a discretized volume with the 3D structural elements in a step-by-step fashion in accordance with a geometrically-based growth law specific for each type of the structure.

In the general case, the design of an artificial 3D-structure includes the following steps. First, the volume to be filled with structural elements is discretized by the computational grid and three-dimensional coordinates are defined for each discrete point. Each cell of the discretized volume is assigned a so-called structural index (SI), which reflects that this point belongs to a certain structural element. Initially, all points possess the same SI equal to zero, which implies an initial homogeneity throughout the volume. At the next step, some cells are assigned specific structural indices different from zero. In such a way, they are treated as nucleating centres (NCs) of new structural elements. At each step in the processing time, the volumes surrounding the nucleating centres are incremented by preset values in accordance with the law of growth. The NCs distribution, the growth law and the increments controlling the growth rate can be derived from the analysis of experimental data, with the parameters can vary for the different structural elements. After the volumes of structural elements have been incremented, for each computational cell with a zero SI so far belonging to none of the structural elements it is checked whether its coordinates fall within any of the volumes. If so, the cell is considered to belong to this structural element and its SI is assigned an appropriate value different from zero. Otherwise it retains the zero SI and is checked again at the next step of the processing time. Such a procedure is repeated until the volume fraction of the growing structural elements has reached the preset magnitude.

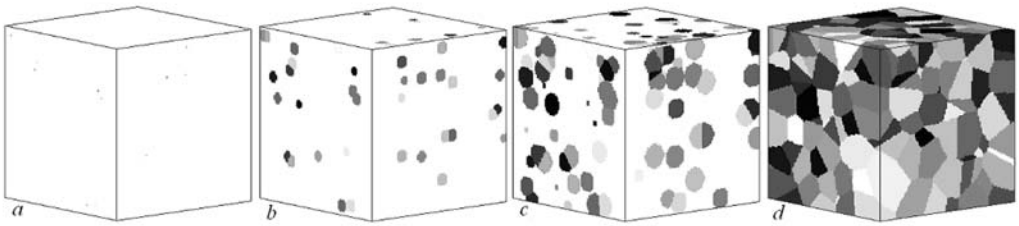

Figure 1. 3D polycrystalline structure at different stages of the SSP-generation procedure; the volume fraction of the structure: 0 (*a*); 10 (*b*); 50 (*c*); 100 % (*d*).

Evidently, each kind of structure requires a special consideration since it is obviously not possible to develop a unified law suitable to design a structure of any sort. As an example let us consider the outlined approach as applied to an idealized case of designing an artificial polycrystalline structure. Figure 1 represents the procedure of polycrystalline structure generation on a grid of 100×100×100. As initial

conditions, 500 nucleation centers were randomly distributed in the volume. In order to avoid the coalescence of grains and formation of elongated structural elements, each nucleation center was assigned SI different from others. For all grains the spherical law and identical rate of growth were preset. On every n-step for all grains the increment radius $R_i^n = R_i^{n-1} + dr_i$, $i = 1, \ldots, 500$, was given. For all cells with zero index the condition

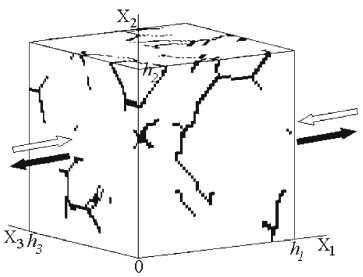

Figure 2. Coal structure and schematics of its loading. White and black arrows show compression and tension, respectively.

$$(X_j - X_i)^2 + (Y_j - Y_i)^2 + (Z_j - Z_i)^2 \le R_i^2 \qquad (8)$$

is then checked by enumeration, where X_j, Y_j, Z_j and X_i, Y_i, Z_i are the coordinates of the j-th cell with $SI(j) = 0$ and i-th grain, respectively. In case if condition (8) is satisfied, the j-th cell is attached to the i-th grain, i.e. $SI(j) = SI(i)$. The criterion for the procedure termination is the absence of cells with zero structural indices in the considered area.

In this paper, calculations for a coal test-piece with an initial crack pattern (Fig. 2) are presented. As the experimental data of Trubitsyn et al. (2002) indicate, physical properties and composition of coals produced in different deposits and lying at different depths are varied in a wide range, with cracks and pores of different scales observed in all coals in more or less degree. Basing on the experimental observations of Trubitsyn et al. (2002), the initial crack pattern has been designed by the SSP-method and introduced explicitly in the 3D calculations. The SSP-algorithm includes two steps – the design of a polycrystalline structure on the grid of 50×50×50 and subsequent erasing a part of the grain boundaries in such a way as to avoid through-the-thickness lines. The remaining boundaries will be further treated as a crack network (plotted in black color in Fig. 2) presenting in a homogeneous base-material (white-colored in Fig.2).

The bulk material is characterized by a homogeneous mechanical properties: density - 1.3 g/cm^3, shear module - 5 GPa, tensile strength - 1.5 MPa, compressive strength - 15 MPa, bulk module - 12.7 GPa. Damaged zones are characterized by a reduced strength and behave themselves in accordance with the fracture model (7).

Specimen size is 500 μm in all three dimensions. Boundary conditions simulating tension and compression as shown in Fig. 2 impling that surfaces $x_2 = 0$, $x_2 = h_2$, $x_3 = 0$ and $x_3 = h_3$ are stress free and surfaces $x_1 = 0$, $x_1 = h_1$ move either towards each other under compression or in the opposite direction under tension (Fig. 2).

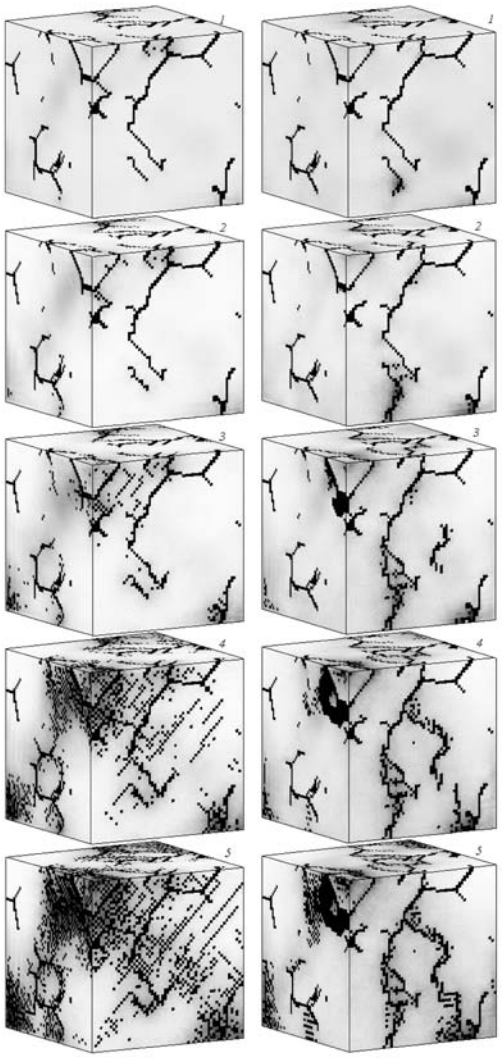

Figure 3. Crack evolution in the coal test-volume subjected to compression (a) and tension (b). Pictures *1-5* correspond to the strain values circled in Fig. 4.

3. Results. As load increases, the fracture criterion is met in local regions producing extended damaged areas that are treated as cracks. Fig. 3 shows crack patterns under compression (a) and tension (b) and stress-strain curves are shown in Fig. 4. Substantial difference in crack behavior under tension and compression is seen.

In contrast with data of Trubitsyn et al (2002) showing 5-7 times difference between coal strength under compression and tension, the curves of Fig. 4 show only two-times difference. This is explained by both scale effects that may be strong for such materials and the assumption of loss of shear strength in damaged areas.

Compression: Under compression (Fig. 3a), new cracks first appear in the undamaged areas of the surface while the reference crack pattern weakly evolves under loading. Analysis shows that surface cracks originate in places whose equivalent stress reaches its tensile strength and where ε_{kk} is positive.

In Fig. 5, solid and open circles show distributions of maximum positive ε_{kk}, and relative volume of the material with $\varepsilon_{kk} > 0$, V_{ten}, in specimen sections $X_3 = const$. These dependencies indicate

that both positive ε_{kk} and volumetric part of tensile areas reach maximum on the surface and subsurface layers. As compressive load is applied on the left and right sides, the top, bottom, front and back surfaces expand, which, along with heterogeneity, contributes to formation of tensile areas near free surfaces. Crack development follows generation of surface waves vanishing at depths of ≈ 30÷50 μm

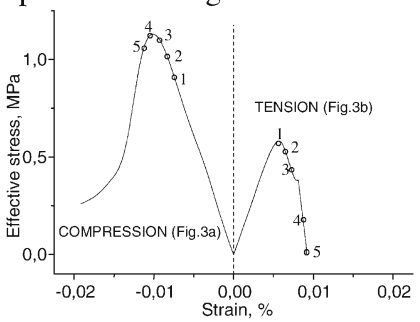

Figure 4. Stress-strain curves of tension and compression. Points 1-5 correspond to pictures in Fig. 3

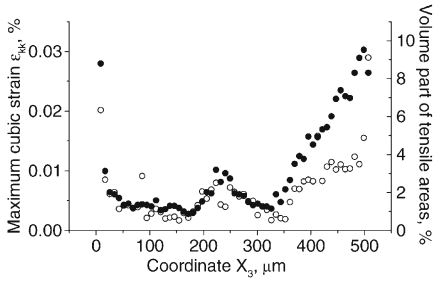

Figure 5. Distribution of maximum positive cubic strain (open circles) and relative volume of tensile areas (solid circles) in sections $X_3 = const$ under compression.

First, cracks form as parallel lines of different lengths oriented at angle ≈45^0 to the axis of loading (pictures 3 and 4 in Fig. 3a) and then originate and propagate in the perpendicular direction (picture 5 in Fig. 3a). Comparison of the crack patterns (Fig. 3a) and the stress-strain curve at compressive loading (Fig. 4) shows that the macroscopic stress starts to decrease as parallel cracks develop. Formation of cracks in the normal direction corresponds to the decreasing part of the curve.

Tension: Fracture process under tensile loading develops on different scenario, Fig. 3b. In contrast to the compression, the initial damage pattern essentially influences crack behavior, i.e. initial cracks under loading start to grow, branching and forming ladder-shaped pattern on the surface.

Comparing Fig. 3b with the tension curve of Fig. 4, the average stress starts to decrease after initial cracks start to grow. Although the rate of decrease is high, the process does not become unstable immediately. A complex crack network impedes the crack propagation. Due to non-homogeneous stress and strain fields associated with both initial heterogeneity and unloading waves, different crack branches develop alternately – one crack stops to grow while the other starts to propagate (pictures 2-4 in Fig. 3). The average stress reduces to zero (point *5* in the tension curve, Fig. 4) when coalescence of the newly-formed cracks results in fragmentation (picture 5 in Fig. 3). This qualitatively agrees with data on coals (Trubitsyn et al, 2002).

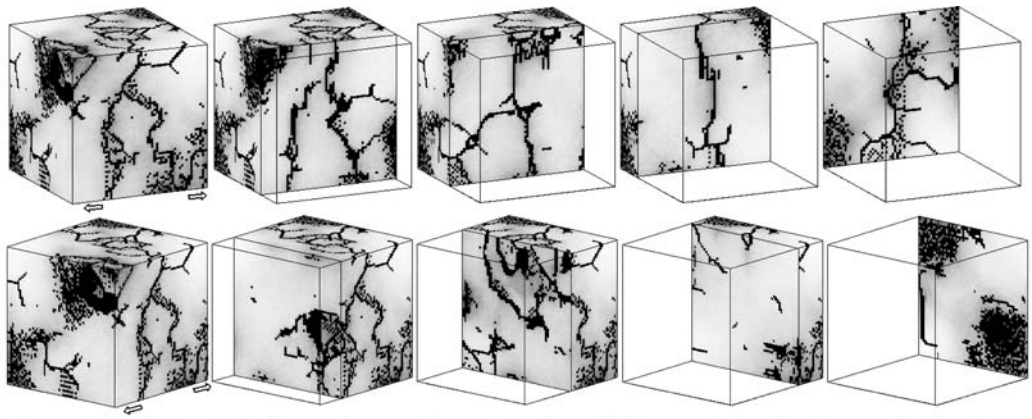

Figure 6. Crack patterns in the specimen sections oriented parallel (upper pictures) and perpendicular (lower pictures) to the axis of tension. Total strain corresponds to point 5 in the stress-strain curve, Fig. 4.

4. Summary. Numerical studies of fracture of coal under tension and compression incorporating 3-D mesostructure combined with the maximum equivalent stress criterion show that the criterion is adequate. Under tensile loading, surface cracks start to grow and propagate inside, resulting in fragmentation. Under compression, new cracks originate in local tensile areas of the surface, forming parallel cracks at the angle of about 45^{o} to the axis of loading. Heterogeneities result in local tensile areas leading to formation of cracks, regardless of macroscopic loading conditions.

Acknowledgments. Support of the Russian-American Program "Basic Research and Higher Education" (TO-016-02) and Russian Foundation for Basic Research (06-01-00592-a) is gratefully acknowledged.

References

Astley, R.J., (1992). Finite elements in solids and structures. *University Press, Cambridge*.

Balokhonov, R., (2005). Hierarchical numerical simulation of nonhomogeneous deformation and fracture of composite materials. *Physical Mesomechanics* **8**, 99-119.

Cherepanov, G.P. (1979). Mechanics of brittle fracture. *McGraw Hill. New York*.

Cherepanov, O.I, (2003) Numerical solution of quasistatic problems in mesomechanics *SB RAS Publ, Novosibirsk*

Jensen, D.J. (2002) Microstructural characterization in 3 dimensions. In R. Pyrz, J. Schjødt-Thomsen, J.C. Rauhe, T. Thomsen and L.R. Jensen (eds.) New Challenges in Mesomechanics: *Proceedings of International Conference, Aalborg, Denmark* 541–547.

Kachanov, L.M. (1974). Basics of fracture mechanics. *Science. Moscow* [in Russian].

Raabe, D., Roters, F., Barlat, F., Chen, L.-Q. (Eds) (2004) Continuum scale simulation of engineering materials. *Wiley-VCH Verlag GmbH & Co*.

Romanova, V., Balokhonov, R, and Karpenko, N., (2004). Numerical simulation of material behavior with explicit consideration for three-dimensional structural heterogeneity. *Physical Mesomechanics* **7**, 71-79 [in Russian]

Romanova, V., Balokhonov, R., Makarov, P., Schmauder, S., and Soppa, E., (2003). Simulation of elasto-plastic behaviour of an artificial 3D-structure under dynamic loading. *Computational Materials Science* **28**, 518-528.

Romanova, V., Soppa, E., Schmauder, S., and Balokhonov, R. (2005). Mesomechanical analysis of the elasto-plastic behavior of a 3D composite-structure under tension. *Computational mechanics* **36**, 475-483.

Trubitsyn, A., Makarov, P., Cherepanov O., et al., (2002). Adaptation of mesomechanical methods to analysis of deformation and fracture in coals. *Kemerovo, Kuzbass-COT* [in Russian].

Wilkins, M., French, S., Sorem, M. (1975) Finite-difference scheme of 3D-spatial and time-dependant problems. *Numerical methods in fluid dynamics. Mir. Moscow* 115-119 [in Russian].